BIOCHEMISTRY
including biophysical chemistry & molecular biology

Article

pubs.acs.org/biochemistry

Identification, Characterization, and Three-Dimensional Structure of the Novel Circular Bacteriocin, Enterocin NKR-5-3B, from *Enterococcus faecium*

Kohei Himeno,[†] K. Johan Rosengren,[‡,§] Tomoko Inoue,[†] Rodney H. Perez,[†] Michelle L. Colgrave,[∥] Han Siean Lee,[‡,§] Lai Y. Chan,[‡] Sónia Troeira Henriques,[‡] Koji Fujita,[†] Naoki Ishibashi,[†] Takeshi Zendo,[†] Pongtep Wilaipun,[⊥] Jiro Nakayama,[†] Vichien Leelawatcharamas,[@] Hiroyuki Jikuya,[#] David J. Craik,[‡] and Kenji Sonomoto*[,†,#]

[†]Department of Bioscience and Biotechnology, Faculty of Agriculture, Kyushu University, 6-10-1 Hakozaki, Higashi-ku, Fukuoka 812-8581, Japan

[‡]Institute for Molecular Bioscience and [§]School of Biomedical Sciences, The University of Queensland, Brisbane, QLD 4072, Australia

[∥]CSIRO Animal, Food & Health Science, Brisbane, QLD 4067, Australia

[⊥]Department of Fishery Products, Faculty of Fisheries, Kasetsart University, Chatuchak, Bangkok 10900, Thailand

[@]Department of Biotechnology, Faculty of Agro-Industry, Kasetsart University, Chatuchak, Bangkok 10900, Thailand

[#]Department of Functional Metabolic Design, Bio-Architecture Center, Kyushu University, 6-10-1 Hakozaki, Higashi-ku, Fukuoka 812-8581, Japan

ABSTRACT: Enterocin NKR-5-3B, one of the multiple bacteriocins produced by *Enterococcus faecium* NKR-5-3, is a 64-amino acid novel circular bacteriocin that displays broad-spectrum antimicrobial activity. Here we report the identification, characterization, and three-dimensional nuclear magnetic resonance solution structure determination of enterocin NKR-5-3B. Enterocin NKR-5-3B is characterized by four helical segments that enclose a compact hydrophobic core, which together with its circular backbone impart high stability and structural integrity. We also report the corresponding structural gene, *enkB*, that encodes an 87-amino acid precursor peptide that undergoes a yet to be described enzymatic processing that involves adjacent cleavage and ligation of Leu[24] and Trp[87] to yield the mature (circular) enterocin NKR-5-3B.

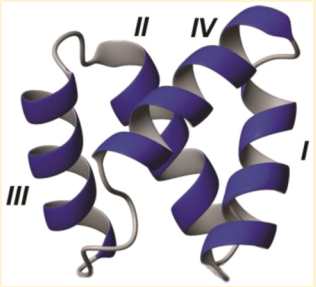

Bacteriocins are antimicrobial peptides ribosomally synthesized by diverse bacteria, including lactic acid bacteria (LAB). Bacteriocins produced by LAB have attracted particular interest because LAB are considered beneficial bacteria and are generally regarded as safe (GRAS).[1,2] LAB bacteriocins have long been proposed as a solution for a myriad of problems involving food contamination, including spoilage and food-borne infection.[3] Furthermore, the growing number of reported LAB bacteriocins having highly potent activities against clinical pathogens, including multidrug resistant (MDR) strains,[4] has motivated the search for novel LAB bacteriocins that can be applied not only as safe food preservatives but also as therapeutic agents.

On the basis of the consensus of their structures and some other features, bacteriocins from LAB and other Gram-positive bacteria are generally divided into two classes, I (lantibiotic) and II (nonlantibiotic), in which class II bacteriocins are further subdivided into four subclasses: pediocin-like bacteriocins (class IIa), two-peptide bacteriocins (class IIb), circular bacteriocins (class IIc), and unmodified, linear, nonpediocin-like bacteriocins (class IId).[3] Among these subclasses, circular bacteriocins have recently gained much attention because of their unique structural features resulting from the head-to-tail cyclization of their backbone.[5−7] As a result of the circular nature of their structures, circular bacteriocins exhibit enhanced stability, not only against thermal and pH stress but also against proteolytic digestion, when compared to their linear counterparts.[8,9] It is also thought that their broader spectrum of antimicrobial activity relative to linear bacteriocins is caused by their cyclic structures.[6,7]

Among the family of bacteriocins, circular bacteriocins are arguably the most poorly understood group. They are synthesized as linear precursor peptides and, like other bacteriocins, contain N-terminal extensions often termed leader peptides.[6] However, unlike the other groups of bacteriocins, their leader peptides show only a low level of sequence homology and vary in length, making it difficult to find a consensus among them. Nevertheless, it has been suggested that circular bacteriocins should be classified on the basis of the length of their leader sequence.[5]

Received: February 25, 2015
Revised: July 14, 2015
Published: July 15, 2015

DOI: 10.1021/acs.biochem.5b00196
Biochemistry 2015, 54, 4863−4876

Since the discovery of the first circular bacteriocin, enterocin AS-48 in 1986,[10] several circular bacteriocins from various bacterial species have been discovered, including gassericin A,[11] subtilosin A,[12] circularin A,[13] butyrivibriocin AR10,[14] uberolysin A,[15] carnocyclin A,[16] lactocyclicin Q,[17] garvicin ML,[18] and most recently leucocyclicin Q.[19] However, among the reported circular bacteriocins, only subtilosin A, enterocin AS-48, and carnocyclin A have three-dimensional (3D) nuclear magnetic resonance (NMR) solution structures. Subtilosin A is atypical because it is significantly shorter than other circular bacteriocins and possesses cross-linkages from three cysteine residues forming individual thioether bridges to two phenylalanine residues and a threonine residue.[12,20] Interestingly, enterocin AS-48 and carnocyclin A, despite sharing only 30% sequence homology and varying in length, display remarkably similar highly compact, globular, and helical structures.[21,22] Surprisingly, despite their difference in length, overall their helical structures align very well. Furthermore, secondary sequence prediction and homology modeling have suggested that other circular bacteriocins share this common structural motif.[22]

Enterococcus faecium NKR-5-3, a thermo-tolerant, salt-tolerant lactic acid bacterium isolated from Thai fermented fish (*Pla-ra*), shows bacteriocin-like activity against various Gram-positive bacteria.[23−26] Purification and mass spectral analysis revealed that *E. faecium* NKR-5-3 produces five bacteriocin peptides, named enterocins NKR-5-3A, -B, -C, -D, and -Z.[24,25] Enterocins NKR-5-3A and -Z were identified as two-peptide components of a class IIb bacteriocin, brochocin C (brochocins A and B, respectively).[27] Enterocin NKR-5-3C was identified as a novel class IIa (antilisterial) bacteriocin.[25] Enterocin NKR-5-3D, belonging to class IId bacteriocins, was found to have weak antibacterial activity but was also able to induce production of the NKR-5-3 enterocins except enterocin NKR-5-3B.[24] In the initial study, the structure of enterocin NKR-5-3B was not further elucidated, but its molecular mass (6316.4 Da) did not resemble those of any reported bacteriocins, suggesting it was novel. Initial attempts to obtain its amino acid sequence by Edman degradation were unsuccessful, indicating that the access to the N-terminal residue was blocked, a typical characteristic of circular bacteriocins.

In this study, we report the characterization and full structure (primary and 3D NMR solution structure) determination of the novel circular bacteriocin, enterocin NKR-5-3B. In addition, we report the identification of the gene encoding enterocin NKR-5-3B, revealing that it is derived from a linear precursor peptide.

EXPERIMENTAL PROCEDURES

Bacterial Strains and Media. *E. faecium* NKR-5-3 was stored at −80 °C in M17 medium (Merck, Darmstadt, Germany) with 15% glycerol and propagated in M17 medium at 30 °C for 22 h before use. Indicator strains for the antimicrobial spectrum were propagated at an appropriate temperature (30 or 37 °C), recommended by the culture collections, for 18 h before use. LAB indicator strains were grown in MRS medium (Oxoid, Basingstoke, U.K.), whereas the other indicator strains were grown in Tryptic Soy Broth (BD, Sparks, MD) supplemented with 0.6% yeast extract (Nacalai Tesque, Kyoto, Japan) (TSBYE). *Escherichia coli* DH5α (Promega, Madison, WI) was cultivated in LB medium (BD) with 1.5% agar containing 50 μg/mL ampicillin.[28]

Purification of Enterocin NKR-5-3B. Enterocin NKR-5-3B was purified from the M17 culture supernatant through a four-step procedure comprising adsorption on Amberlite XAD-16 resin, SP-Sepharose cation exchange chromatography, Octyl-Sepharose hydrophobic interaction chromatography, and finally reverse-phase high-performance liquid chromatography (HPLC), as described previously.[24] Solvents in the purified fraction were removed by lyophilization. Purified bacteriocin dissolved in 0.1% (v/v) Tween 80 was used for MIC determination and other assays unless specified otherwise.

Antibacterial Activity Assay. Bacteriocin activities were determined using the spot-on-lawn method.[29] Briefly, 10 μL of 2-fold dilutions of the bacteriocin preparation in 0.1% Tween 80 aqueous solution was spotted onto a double layer composed of 7 mL of Lactobacilli Agar AOAC (BD) with a 70 μL culture of an indicator strain (~10^7 colony-forming units/mL) as the top layer and 10 mL of MRS medium supplemented with 1.2% agar as the bottom layer. After overnight incubation, the bacterial lawns were checked for inhibition zones. The minimum inhibitory concentrations (MICs) of enterocin NKR-5-3B were defined as the minimum concentrations that yielded clear zones of growth inhibition in the indicator lawns. All assays were performed in triplicate.

Characterization of the Stability of Enterocin NKR-5-3B. Tests of the stability of enterocin NKR-5-3B were performed as described previously.[17] Purified enterocin NKR-5-3B was resuspended in appropriate buffers between pH 2.0 and 10.0. For the pH stability assays, the preparations at each pH were kept at room temperature overnight, and the pH was readjusted to 6.0 so the residual activity could be compared with that of the preparation at pH 5.0 without incubation. For the heat stability assays, the preparations at each pH were heated at 80, 100, or 121 °C for 15 min, and the residual activity was compared with the activity without heat treatment at the respective pH. The residual bacteriocin activities were determined as described above employing *Lactococcus lactis* subsp. *lactis* ATCC 19435^T as an indicator strain. All tests were performed in triplicate.

Edman Degradation Sequencing. The N-terminal amino acid sequence of enterocin NKR-5-3B was analyzed on the basis of Edman degradation with a protein sequencer model PPSQ-21 (Shimadzu, Kyoto, Japan). Enterocin NKR-5-3B treated with BNPS-skatole [3-bromo-3-methyl-2-(2-nitrophenylthio)-3*H*-indole] was also analyzed. BNPS-skatole treatment, which cleaves on the C-terminal side of tryptophan residues, was conducted according to procedures previously reported,[17] and the resulting peptide fragment was purified by reverse-phase HPLC, as described previously.[24]

Enzymatic Digestion. An aliquot containing ~5 μg of enterocin NKR-5-3B was dissolved in 20 μL of 100 mM ammonium bicarbonate buffer (pH 8.5) and digested using either trypsin or chymotrypsin. Sequencing grade trypsin (Promega) or chymotrypsin (Sigma-Aldrich, Steinheim, Germany) was added at a 1:20 ratio. After enzymatic digestion overnight at 37 °C, an equal volume of 1% formic acid was added and the sample was stored at 4 °C prior to liquid chromatography−tandem mass spectrometry (LC−MS/MS) analyses.

Matrix-Assisted Laser Desorption Ionization Time-of-Flight (MALDI-TOF) MS Analysis. MALDI-TOF analyses were conducted using an Applied Biosystems (Foster City, CA) 4700 TOF-TOF Proteomics Analyzer. Samples were prepared at a 1:1 dilution, with a matrix consisting of 5 mg/mL α-cyano-

DOI: 10.1021/acs.biochem.5b00196
Biochemistry 2015, 54, 4863−4876

4-hydroxycinnamic acid (CHCA) in 50% (v/v) acetonitrile and 1% (v/v) formic acid, prior to spotting on a stainless steel MALDI target. MALDI-TOF spectra were acquired in reflector positive operating mode with the source voltage set at 20 kV and the Grid1 voltage at 12 kV, a mass range of m/z 1000−5000, and a focus mass of m/z 1500, collecting 1500 shots using a random laser pattern and with a laser intensity of 3500. External calibration was performed by spotting a 1:1 CHCA matrix with an Applied Biosystems Sequazyme PeptideMass Standards Kit calibration mixture diluted 1:400, as described previously.[30]

Nanospray Analysis. Enzymatically digested samples were processed using C18 ziptips (Millipore, Billerica, MA) to remove salts and elicit a solvent exchange from an aqueous solution to 80% (v/v) acetonitrile and 1% (v/v) formic acid. Samples (3 μL) were introduced to nanospray tips (Proxeon ES380, ThermoScientific, West Palm Beach, FL), and 900 V was applied to the tip to induce nanoelectrospray ionization on a QSTAR Pulsar I QqTOF mass spectrometer (Applied Biosystems). The collision energy was varied from 10 to 60 V. Both TOF and product ion mass spectra were acquired and manually assigned using Analyst QS 1.1.

LC−MS/MS Analysis. Each sample (4 μL) was dissolved in 1% formic acid (aqueous) and injected onto an Agilent 1100 Binary HPLC system (Agilent, Santa Clara, CA) at a flow rate of 4 μL/min onto a Vydac MS C18 300 Å, column (150 mm × 2 mm) with a particle size of 5 μm (Grace Davison, Deerfield, IL). Chromatographic separation was achieved using a linear gradient of 2 to 42% solvent B over 40 min. The mobile phases consisted of solvent A (0.1% formic acid) and solvent B (0.1% formic acid, 90% acetonitrile, and 10% water). The HPLC eluent was coupled directly to a QStar Elite Hybrid LC/MS/MS system (Applied Biosystems) with a nanoelectrospray ionization source. Source conditions included an ion spray voltage of 4200 V, a nebulizer gas flow of 30, a curtain gas flow of 20, and an interface heater temperature of 140 °C, and collision-induced dissociation settings included CAD gas set to 5 and a declustering potential of 70 V. The MS/MS data-dependent acquisition mode was used, in which survey MS spectra were collected (m/z 350−1800) for 1 s followed by three MS/MS measurements using an accumulation time of 2 s for each on the three most intense parent ions (50 counts/s threshold, +2 to +5 charge state, and mass range of m/z 100−1800 for MS/MS). Parent ions targeted previously were excluded from repetitive MS/MS acquisition for 30 s (mass tolerance of 250 mDa). Data were acquired and processed using Analyst QS 2.0.

Database Searching with ProteinPilot. ProteinPilot 2.0.1 (Applied Biosystems), with the Paragon Algorithm, was used for the identification of proteins. MS/MS data were searched against a custom-built database composed of the Swissprot database (release date, May 2010) and including the enterocin NKR-5-3B sequence as determined by *de novo* sequencing. Search parameters were defined as cysteine alkylation with iodoacetamide, trypsin, or chymotrypsin as the digestion enzyme, and no restrictions were placed on taxonomy. Single-amino acid substitutions were allowed in the preliminary iterations of database searching. Modifications were set to the "generic workup" and "biological" modification sets provided with this software package, which consisted of 126 possible modifications, including acetylation, methylation, and phosphorylation. The generic workup modification set contains 51 potential modifications that may occur as a result of sample handling, for example, oxidation, dehydration, and deamidation. The criterion for a positive protein identification was a full-length peptide with ≥95% confidence (score of >1.3). All matching spectra were manually validated.

NMR Spectroscopy. The samples prepared for solution NMR spectroscopy contained 3 mg of enterocin NKR-5-3B dissolved in 0.5 mL of H_2O/10% D_2O or 100% D_2O at pH ∼5.0. Data were recorded in the temperature range of 17−37 °C on Bruker Avance 600 MHz and Bruker Avance II 900 MHz NMR spectrometers, both equipped with cryoprobes. Homonuclear $^1H-^1H$ two-dimensional (2D) data recorded included TOCSY with a mixing time of 80 ms, NOESY with a mixing time of 100 or 150 ms, and DQF-COSY. These data sets were all recorded with 4K data points in the direct dimension and 512 increments in the indirect dimension over a spectral width of 12 ppm. Water suppression was achieved using excitation sculpting. In addition, heteronuclear $^1H-^{13}C$ HSQC and $^1H-^{15}N$ HSQC data were recorded at natural abundance. All spectra were referenced directly or indirectly to DSS at 0 ppm.

3D Structure Determination. Data were analyzed and assigned using CARA.[31] For the structure determination, restraints were derived from the NMR data. These included interproton distance restraints based on NOESY cross-peak volumes and backbone ϕ and ψ and side chain χ^1 dihedral angles derived from a TALOS-N[32] analysis of HN, Hα, Cα, Cβ, and N chemical shifts determined from HSQC data. Hydrogen bond restraints were included for amide protons that were identified as being involved in hydrogen bonds in the deuterium exchange experiment, and for which unambiguous acceptors could be identified in the preliminary structures.

NOESY assignments and initial structures were generated using torsion angle dynamics and the automated assignment module of CYANA.[33] Final structures were generated using Cartesian dynamics and refinement and energy minimization within CNS,[34] using protocols from the RECOORD database.[35] Final structures were analyzed using MOLPROBITY[36] and figures prepared using MOLMOL.[37] The coordinates and NMR assignments for enterocin NKR-5-3B have been deposited in the Protein Data Bank and BioMagResBank as entries 2mp8 and 19970, respectively.

DNA Sequencing Analysis of the Structural Gene. To clone the gene (*enkB*) encoding the enterocin NKR-5-3B precursor peptide, polymerase chain reaction (PCR) and DNA sequencing were performed using the primers listed in Table 1, and *E. coli* DH5α was used as a cloning host strain. Total DNA was extracted from *E. faecium* NKR-5-3, as previously described.[38] The total DNA was digested with *Bam*HI, *Eco*RI, *Hin*dIII, *Kpn*I, *Spe*I, or *Xba*I (Nippon Gene, Tokyo, Japan), and

Table 1. Oligonucleotide Primers Used To Clone the Structural Gene of Enterocin NKR-5-3B (*enkB*)

primer name	corresponding amino acid sequence	sequence (5′−3′)
Bd-F1	TANLGI	ACNGCNAAYYTNGGNATH
Bd-F2	YAAKKVI	TAYGCNGCNAARAARGTNAT
Bd-F3	IKKYGAK	ATHAARAARTAYGGNGCNAA
Bd-R1	IKKYGAK	TTNGCNCCRTAYTTYTTDAT
Bd-R2	YAAKKVI	ATNACYTTYTTNGCNGCRTA
Bd-R3	TANLGI	DATNCCNARRTTNGCNGT
PB-F1		GATGAACCTGCTTTCTCACC
PB-R1		CGACTTGATAGTCGCCTTTA

DOI: 10.1021/acs.biochem.5b00196
Biochemistry 2015, 54, 4863−4876

the digested DNA was ligated into a pUC18 cloning vector (Toyobo, Osaka, Japan) treated with the corresponding restriction enzymes and then dephosphorylated. Each of the various ligation products was used as a template for PCR. To obtain the *enkB* gene, the degenerate primers (Bd-F1, Bd-F2, and Bd-F3) were designed on the obtained amino acid sequence and vector specific primers for ligation-anchored and nested PCR. To amplify the upstream region of *enkB*, the degenerate primers (Bd-R1, Bd-R2, and Bd-R3) were designed. The obtained fragments were purified using a QIAquick PCR purification kit (Qiagen, Hilden, Germany) and sequenced. The amplified fragments were cloned and sequenced, and then a new set of specific primers (PB-F1 and PB-R1) was designed to confirm the DNA sequence of *enkB* and its vicinity. DNA sequencing was conducted by Fasmac (Kanagawa, Japan). The obtained DNA sequence was analyzed using BLAST of NCBI (http://www.ncbi.nlm.nih.gov/) and has been deposited in the DNA Data Bank of Japan as entry AB908993.

Serum Stability. To test its ability to resist degradation under relevant biological conditions, enterocin NKR-5-3B was incubated in human serum from male AB plasma (Sigma-Aldrich) at an initial concentration of 200 μM. The amount of peptide remaining at incubation time points of 0, 4, 8, 16, and 24 h was determined by UHPLC analysis. Sample preparations were as described previously;[39] 50 μL of the supernatant was taken out in triplicate from each time point and chromatographed on a Nexera UHPLC instrument (Shimadzu) with a flow rate of 0.4 mL/min on a 0.8 mL/min Agilent column using a 2% gradient from 0 to 50% solvent B. The elution time for enterocin NKR-5-3B was determined by the serum control at time zero. The stability of enterocin NKR-5-3B at each time point was calculated as the height of the serum-treated peptide peak on UHPLC at 215 nm as a percentage of the height of the zero-hour serum-treated control. The experiment was conducted in triplicate.

Hemolytic Assay. Human red blood cells were used to measure the ability of enterocin NKR-5-3B to lyse human cells. Melittin, a 26-amino acid well-known strongly hemolytic peptide and the principle active component of bee venom, was used as a positive control in this experiment; 300 μM enterocin NKR-5-3B and 20 μM melittin were used as the highest concentrations to prepare 2-fold serial dilutions with eight concentrations in total. Hemolytic activity was monitored via the absorbance at 415 nm using a BioTek PowerWave XS spectophotometer, as described previously.[39]

Interaction of Enterocin NKR-5-3B with Model Membranes. Synthetic lipids [palmitoyloleoylphosphatidylcholine (POPC), palmitoyloleoylphosphatidylglycerol (POPG), palmitoyloleoylphosphatidylethanolamine (POPE), cholesterol (Chol), cardiolipin (CL), and extracted sphingomyelin (SM) from porcine brain, which contains 50% C(18:0), 21% C(24:1), 2% C(16:0), 5% C(20:0), 7% C(22:0), and 5% C(24:0)] and *E. coli* polar lipid extract (containing 67% PE, 23.2% PG and 9.8% CL, w/w) were obtained from Avanti Polar Lipids and used to prepare model membranes.

The interaction of enterocin NKR-5-3B with model membranes was followed by surface plasmon resonance (SPR) with an L1 chip sensor and a Biacore 3000 instrument (GE Healthcare), using methodologies previously described.[40] Briefly, small unilamellar vesicles with a diameter of 50 nm and a POPC/Chol/SM (1:1:1 molar ratio), POPE/POPG (7:3 molar ratio), or POPG/CL (6:4 molar ratio) composition were prepared by extrusion and deposited onto an L1 chip sensor. The peptide at concentrations ranging from 1 to 64 μM was injected over deposited membranes. All the solutions were freshly made filtered with a 0.22 nm filter; 10 mM HEPES buffer containing 150 mM NaCl was used to prepare all the solutions and as a running buffer.

RESULTS

Antimicrobial Activity and Characteristics of Enterocin NKR-5-3B. Purified enterocin NKR-5-3B showed antimicrobial activity against a wide range of Gram-positive indicator strains (Table 2). In particular, it showed highly specific activities (low MICs) against strains of *Bacillus* and *Enterococcus*, strains usually associated with food spoilage. However, enterocin NKR-5-3B showed no activity against Gram-negative bacteria such as *E. coli* and *Salmonella*, as is the case with most bacteriocins from Gram-positive bacteria. Furthermore, it retained almost full antimicrobial activity after overnight treatments over the pH range of 2−6. In addition, the activity was stable even after a 15 min heat treatment at 80 °C over the pH range of 2−10.

Table 2. Antibacterial Spectrum of Enterocin NKR-5-3B

indicator strain	MIC (μM)[a]
Gram-Positive	
Lactococcus lactis ssp. *lactis* ATCC 19435^T	0.290
L. lactis ssp. *lactis* IL1403	0.0490
L. lactis ssp. *cremoris* NZ9000	0.719
L. lactis ssp. *lactis* JCM 7638	0.078
Lactococcus sp. QU 12	5.75
Lactobacillus sakei ssp. *sakei* JCM 1157^T	0.570
Lactobacillus plantarum ATCC 14917^T	1.14
Leuconostoc mesenteroides ssp. *mesenteroides* JCM 6124^T	0.781
Leu. mesenteroides TK41401	0.359
Pediococcus pentosaceus JCM 5890^T	0.570
Pediococcus dextrinicus JCM 5887^T	0.0390
Enterococcus faecium JCM 5804^T	0.195
Enterococcus faecalis JCM 5803^T	1.14
E. faecalis NKR-4-1	0.359
E. faecalis JH-2-2	1.44
E. faecium NKR-5-3	5.75
Streptococcus bovis JCM 5802^T	1.44
Streptococcus mutans JCM 5707^T	NA (>200)
Bacillus coagulans JCM 2257^T	0.290
Bacillus circulans JCM 2504^T	0.290
Bacillus subtilis JCM 1465^T	0.570
Kocuria rhizophila NBRC 12708	1.14
Listeria innocua ATCC 33090^T	2.29
Listeria monocytogenes ATCC BAA-679	0.693
Staphylococcus aureus ssp. *aureus* ATCC 12600^T	NA (>184)
Staphylococcus epidermidis JCM 2414^T	0.391
Gram-Negative	
Salmonella typhimurium NBRC 13245	NA (>184)
Escherichia coli JM109	NA (>200)
E. coli DH5α	NA (>200)

[a]Abbreviations: MIC, minimum inhibitory concentration; NA, no activity at the highest concentration tested shown in parentheses. The MIC values were based on the quantified concentration of purified enterocin NKR-5-3B.

Edman Degradation Sequencing. Enterocin NKR-5-3B was isolated and purified together with another four NKR-5-3 enterocins.[24] When enterocin NKR-5-3B was directly subjected

DOI: 10.1021/acs.biochem.5b00196
Biochemistry 2015, 54, 4863−4876

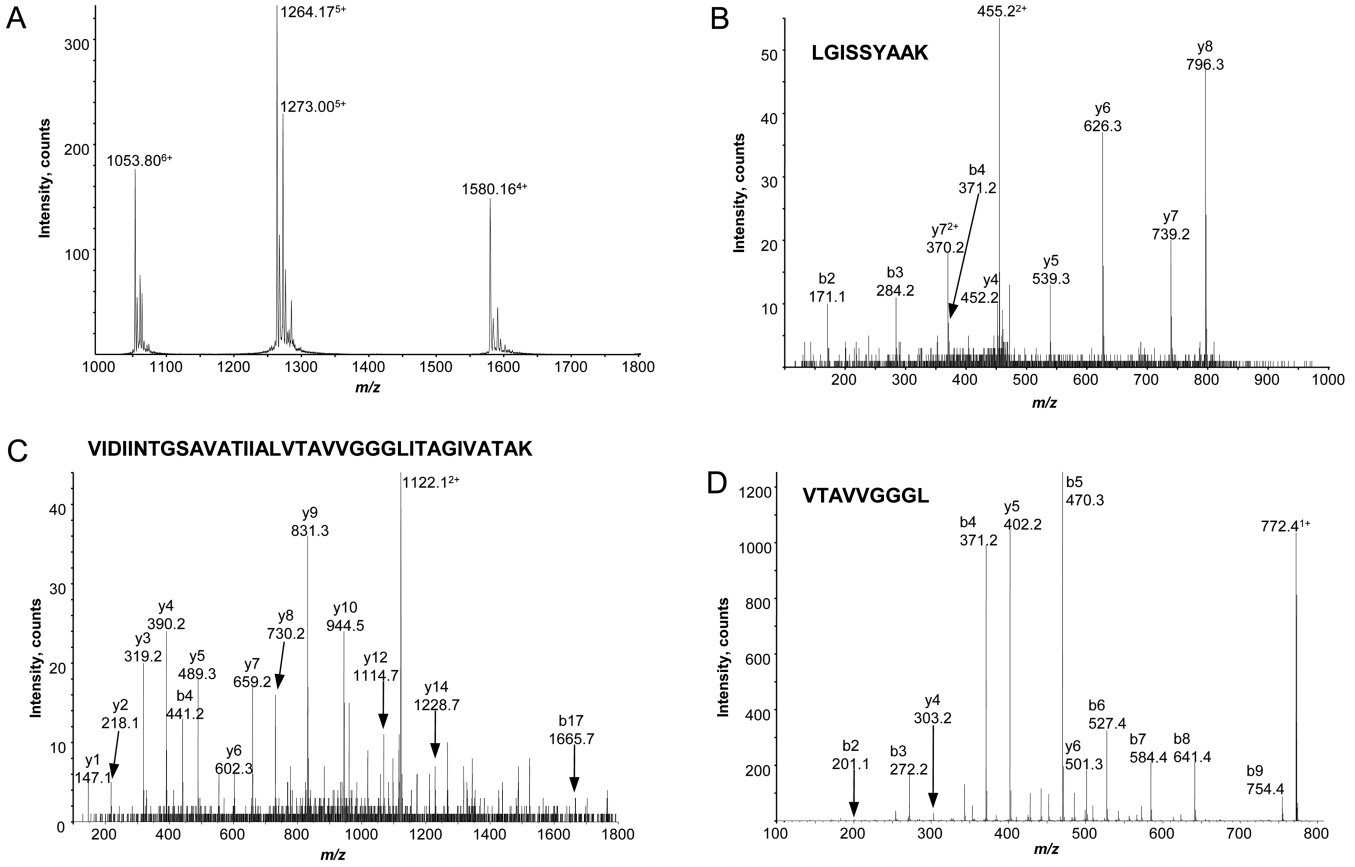

Figure 1. Mass spectra of native enterocin NKR-5-3-B. (A) Nanoelectrospray TOF MS. The experimentally determined average m/z values were 1053.80^{6+}, 1264.17^{5+}, and 1580.16^{4+}, corresponding to an average molecular weight of 6316.42 (theoretical mass of 6316.54 with a mass error of 18 ppm). (B–D) MS/MS sequencing of enterocin NKR-5-3B. Product ion MS/MS spectrum for trypsin digestion of enterocin NKR-5-3B: (B) LGISSYAAK at m/z 455.20 (t_R = 8.5 min) and (C) VIDIINTGSAVATIIALVTAVVGGGLITAGIVATAK at m/z 1121.57 (t_R = 40.6 min). Product ion MS/MS spectrum for chymotrypsin digestion of enterocin NKR-5-3B: (D) VTAVVGGGL at m/z 772.29 (t_R = 15.2 min).

to Edman degradation sequencing, no sequence was obtained, probably because of the modified N-terminal amino acid residue. Moreover, when the sample was subjected to treatment with BNPS-skatole, a peptide cleavage reagent specific for the carboxyl side of tryptophan residues, a 112 Da increase in molecular mass was observed, a likely result of hydrolysis, bromination, and oxidation reactions. For linear peptides, treatment with a cleavage reagent or enzyme would be expected to yield peptide fragments with molecular masses lower than that of the native peptide. The aforementioned increase in molecular mass indicates that enterocin NKR-5-3B contains a single tryptophan residue and a circular structure probably resulting from head-to-tail linkage of the N- and C-termini. Furthermore, Edman degradation sequencing of the peptide fragment obtained after BNPS-skatole treatment revealed the partial amino acid sequence LTANLGISSYAAKKVIDIINTGS. The estimated mass of this sequence is very much lower than the observed mass of enterocin NKR-5-3B (see below), which indicated the sequence obtained was incomplete.

Mass Spectrometry. Enterocin NKR-5-3B was analyzed by a suite of mass spectrometric approaches. The native peptide was examined by MALDI-TOF MS and nanospray ESI-MS, revealing a peptide with a molecular mass of 6316.42 Da. Figure 1A shows the nanospray ESI-MS spectrum, with major peaks at m/z 1053.80, 1264.17, and 1580.16 representing the 6+, 5+, and 4+ charge states of the peptide corresponding to a mass of 6316.42 Da.

Peptides resulting from tryptic digestion were subjected to manual *de novo* sequencing. Figure 1B–D shows three representative spectra that allowed the elucidation of the peptide sequence. Figure 1B revealed the sequence LGISSYAAK. This peptide was observed in the tryptic digest and is somewhat unusual in that it is semitryptic. Trypsin is expected to cleave at the C-terminal side of Lys and Arg. The peptide is cleaved at a C-terminal Lys, but in the mature peptide, the residue preceding the N-terminal Leu is in fact an Asn. Figure 1C reveals the sequence VIDIINTGSAVATIIALVTAVVGGGLITAGIVATAK. This 36-amino acid peptide is fully tryptic, cleaved by trypsin at both ends. Subsequently, enterocin NKR-5-3B was subjected to chymotrypsin digestion. Figure 1D shows a representative spectrum of a chymotryptic peptide. Manual *de novo* sequencing revealed the sequence VTAVVGGGL, wherein the peptide has been cleaved at Leu residues at both termini, an expected result for chymotrypsin digestion.

In parallel, the peptide digests were analyzed by online nanoLC-MS/MS on a QStar Elite mass spectrometer. The spectral data sets were searched against the subset of the Uniprot database composed of proteins annotated as bacteriocins using the ProteinPilot search engine. A single peptide (IGISSYAAK) mapping to the circular bacteriocin (Uniprot entry trlE4JJJ4) was detected in the tryptic digest. Subsequently, the spectral data set was searched against the Swissprot database to which the putative enterocin NKR-5-3B sequence as determined by manual *de novo* sequencing had

DOI: 10.1021/acs.biochem.5b00196
Biochemistry 2015, 54, 4863–4876

Table 3. Peptides Identified by LC−MS/MS[a]

time	Sc	contrib	conf	sequence	prec m/z	z	prec MW	theor MW	Δmass
				(A) Tryptic Peptides Identified by LC−MS/MS: Protein Score, 22.32; Sequence Coverage, 80%					
13.63	14	2.00	99	TANLGISSY	463.19	2	924.37	924.46	−0.086
9.94	13	2.00	99	TANLGISSYAAK	598.27	2	1194.52	1194.62	−0.108
40.37	29	2.00	99	TGSAVATIIALVTAVVGGGLITAGIVATAK	899.13	3	2694.38	2694.59	−0.213
18.80	18	2.00	99	VIDIINTGSAVA	586.76	2	1171.51	1171.64	−0.139
18.48	19	2.00	99	VIDIINTGSAVAT	637.29	2	1272.57	1272.69	−0.123
31.48	25	2.00	99	VIDIINTGSAVATIIAL	842.43	2	1682.85	1682.98	−0.136
43.23	18	2.00	99	VIDIINTGSAVATIIALVTAVVGGGLITAGIVAT	1055.25	3	3162.73	3162.85	−0.120
40.91	23	2.00	99	VIDIINTGSAVATIIALVTAVVGGGLITAGIVATAK	841.53	4	3362.10	3361.98	0.117
8.48	14	1.47	99	LGISSYAAK	455.20	2	908.39	908.50	−0.105
14.38	15	1.39	99	GLITAGIVATAK	557.75	2	1113.49	1113.68	−0.181
12.22	15	1.12	99	LITAGIVATAK	529.28	2	1056.55	1056.65	−0.102
16.64	13	0.74	99	VIDIINTGSA	501.72	2	1001.43	1001.54	−0.110
14.45	14	0.71	99	GGLITAGIVATAK	586.31	2	1170.60	1170.70	−0.094
17.34	13	0.56	99	YAAAWLTAN	490.69	2	979.37	979.48	−0.107
				(B) Chymotryptic Peptides Identified by LC−MS/MS: Protein Score, 92.33; Sequence Coverage, 97%					
16.25	14	2.00	99	TANLGISSY	463.242	2	924.47	924.46	0.014
23.57	14	2.00	99	LTANLGISSY	519.778	2	1037.54	1037.54	0.003
47.57	39	2.00	99	AAKKVIDIINTGSAVATIIALVTAVVGGGLITAGIVATAKSL	991.101	4	3960.37	3960.36	0.014
47.14	23	2.00	99	AAKKVIDIINTGSAVATIIALVTAVVGGGLITAGIVATAKSLIKKY	899.554	5	4492.73	4492.70	0.036
46.40	18	2.00	99	AAKKVIDIINTGSAVATIIALVTAVVGGGLITAGIVATAKSLIKKYGAKY	819.669	6	4911.97	4911.92	0.058
36.11	17	2.00	99	VTAVVGGGLITAGIVATAKSL	633.391	3	1897.15	1897.13	0.026

[a]Abbreviations: Sc, protein score; contrib, peptide contribution to protein score; conf, confidence; prec m/z, precursor mass-to-charge ratio; z, charge; prec MW, precursor molecular weight; theor MW, theoretical molecular weight.

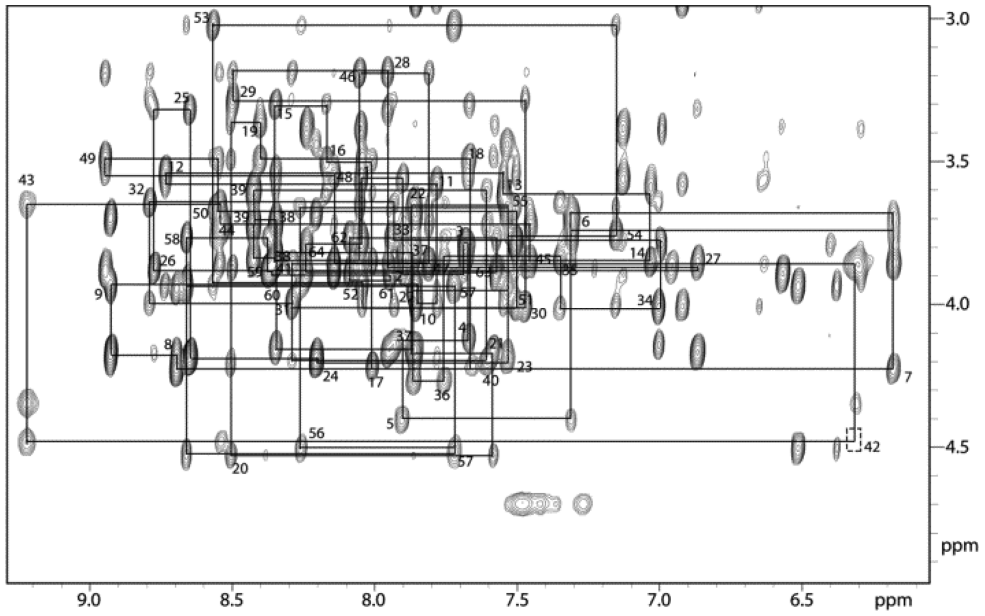

Figure 2. NOESY spectrum of enterocin NKR-5-3B. The spectrum was recorded at 900 MHz, 298 K, and pH 5 with a mixing time of 150 ms. The "sequential walk" of Hα−HN NOE connections throughout the entire sequence, including between Trp^{64} and Leu^{1}, highlight the quality of the data and confirm the presence of a circular backbone.

been appended. Table 3 shows the peptides identified by ProteinPilot.

NMR Spectroscopy and Structure Determination. For the structural analysis using solution NMR spectroscopy, a sample containing 3 mg of enterocin NKR-5-3B dissolved in 0.5 mL of water was prepared and extensive homonuclear ^{1}H 2D NMR spectra, including TOCSY, NOESY, and DQF-COSY spectra, were recorded in the temperature range of 17−37 °C at 600 and 900 MHz. The spectral data were of excellent quality, with sharp and well-dispersed signals, allowing complete resonance assignments of the peptide backbone and most side chains to be achieved using standard 2D homonuclear assignment strategies. The fingerprint region of a NOESY spectra recorded at 900 MHz with a continuous sequential walk from residue 1 to 64, including NOEs between Trp^{64} and Leu^{1} confirming the presence of a circular backbone, is shown in Figure 2. No significant line broadening or minor conformations were observed, confirming that enterocin NKR-5-3B adopts a single well-ordered conformation in solution.

Strong NH−NH sequential NOEs were observed throughout most of the sequence, which is consistent with the majority of the secondary structure being helical. This observation was

DOI: 10.1021/acs.biochem.5b00196
Biochemistry 2015, 54, 4863−4876

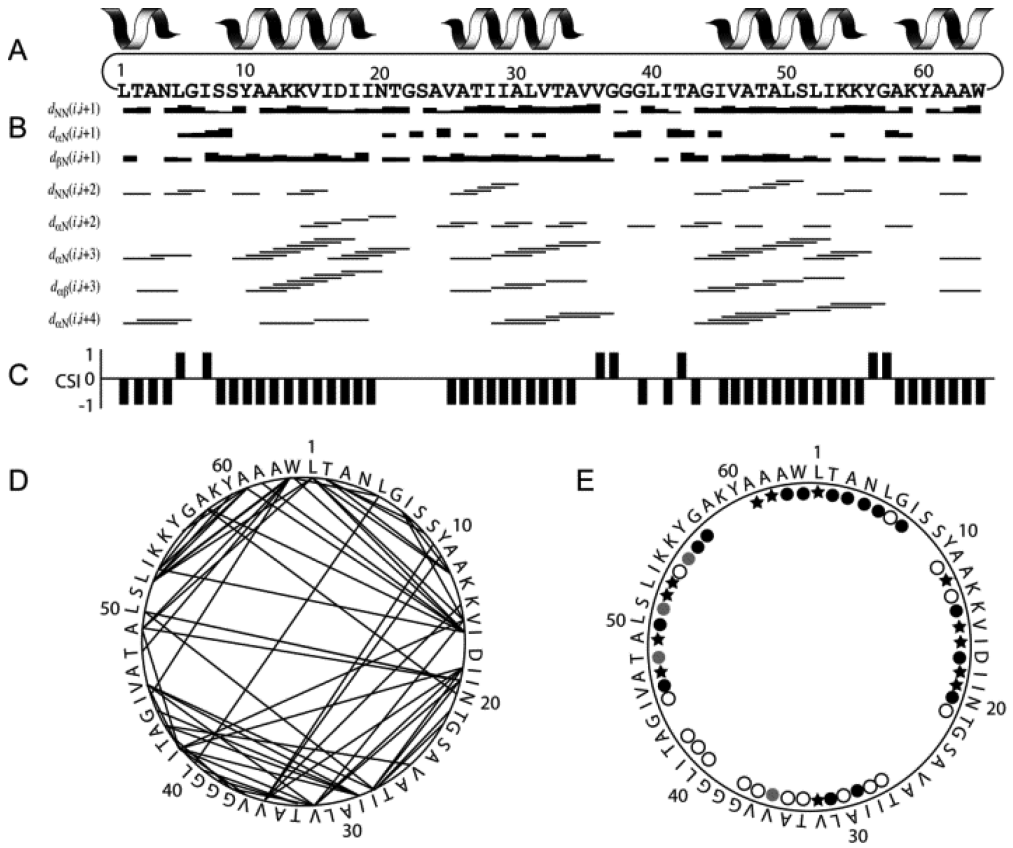

Figure 3. NMR structural data for enterocin NKR-5-3B. (A) Primary sequence with a line highlighting the cyclic backbone and schematic helices indicating the helical regions. (B) Observed sequential and medium-range NOEs defining the helical segments. The thickness of the bar corresponds to the intensity of the sequential NOEs. (C) The chemical shift index is the difference in observed Hα chemical shifts minus random coil chemical shifts.[53] Possible values of the CSI are 1 (for Hα-RC of >0.1 ppm), 0 (for Hα-RC between 0.1 and −0.1 ppm), and −1 (for Hα-RC of <0.1 ppm). Stretches of values of 1 or −1 are indicative of sheets or helices, respectively. (D) Patterns of observed long-range NOE contacts are shown as lines connecting residues that have at least one NOE between them. (E) Amide exchange rates for amide protons. Residues still visible after 1 h in D_2O are denoted by a white circle, after 12 h by a gray circle, and after 24 h by a black circle. Amide protons still visible after storage in 100% D_2O for 4 years are denoted by black stars.

confirmed both by analysis of the Hα chemical shifts, which were generally upfield-shifted, and by the identification of a large number of medium-range NOEs clearly defining four helical segments comprising residues 9−21, 25−36, 43−55, and 58−65. Furthermore, deuterium exchange experiments were conducted to identify hydrogen-bonded amide protons. A large number of amide protons were still visible after 12−24 h, suggesting the structure is stabilized by a large number of hydrogen bonds. After the initial study of enterocin NKR-5-3B was finalized, the sample was left in a deuterium solution in the refrigerator for 4 years, after which some additional NMR data were recorded. Remarkably, the peptide was completely intact, showing no signs of degradation, and 13 amide protons had not been fully exchanged and were still visible, highlighting the extreme stability and rigidity of the fold. A summary of the raw NMR data, including sequential, medium-range, and long-range NOEs, as well as amide exchange and secondary shifts, is presented in Figure 3.

For the structure determination of enterocin NKR-5-3B, cross-peak intensities from the NOESY spectrum, coupling constants derived from the DQF-COSY spectrum, and information on slowly exchanging amides derived from deuterium exchange experiments were translated into inter-proton distance restraints, dihedral angle restraints, and hydrogen bond restraints, respectively. This information was subsequently used as input for structure calculations using torsion angle simulated annealing followed by refinement and energy minimization in explicit solvent. Preliminary structures were used to guide the assignment of NOEs that were ambiguous because of chemical shift overlaps and for the identification of hydrogen bond acceptors for slowly exchanging amides. For the final round, a set of 50 structures was calculated using a total of ∼1200 restraints and the 20 structures with the lowest energy chosen to represent the solution structure of enterocin NKR-5-3B.

An overlay of the calculated structures is presented in Figure 4. From this overlay, it is clear that enterocin NKR-5-3B forms a well-defined structure throughout most of the peptide sequence, with the only mildly disordered regions seen in loops 22−24 and 37−42. Both these loops are classified as dynamic by TALOS-N based on their chemical shift patterns[32,41] and have predicted order parameters (S^2) of ∼0.5, whereas the remaining residues are all highly structured with predicted order parameters of 0.85−0.9. The residue 37−42 loop incorporates a triple-Gly motif at positions 37−39, which likely contributes to its flexibility. The structure is in excellent agreement with both experimental data and ideal covalent geometry, as is evident from minimal violations of experimental restraints and a MOLPROBITY analysis, presented in Table 4.

DOI: 10.1021/acs.biochem.5b00196
Biochemistry 2015, 54, 4863−4876

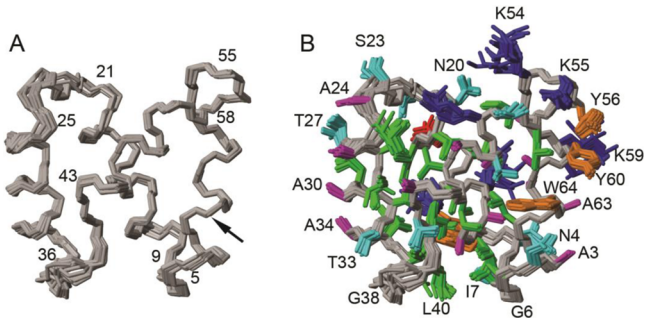

Figure 4. Overlay of the calculated 3D solution structure of enterocin NKR-5-3B. (A) The superposition of the backbone highlights the well-defined fold and the highly ordered helical segments. Disorder is seen only in the loops comprising residues 22−24 and 37−42, which are both confirmed to be flexible based on chemical shifts. The first and last residues of each helical segment are numbered. An arrow indicates the peptide bond between Trp^{64} and Leu^{1}. (B) The high definition of the heavy atoms of the side chains further highlights the compact fold and efficient packing of the hydrophobic core. Hydrophobic residues (Val, Ile, and Leu) are colored green, hydrophilic residues (Ser, Thr, and Asn) aqua, positively charged residues (Lys) blue, negatively charged residues (Asp) red, aromatic residues (Trp, Tyr) orange, and Ala residues pink. Selected residues are labeled with single-amino acid codes and residue numbers.

Description of the 3D Structure of Enterocin NKR-5-3B. The structure of enterocin NKR-5-3B is characterized by four helical segments that enclose a tightly packed hydrophobic core, which together with the circular backbone is the main stabilizing feature of the fold. The core primarily comprises the hydrophobic side chains of residues Leu^{1}, Leu^{5}, Ile^{7}, Ala^{12}, Val^{15}, Ile^{16}, Ile^{18}, Ile^{19}, Ile^{28}, Val^{32}, Ile^{41}, Ile^{45}, Val^{46}, Ala^{49}, Leu^{52}, Ile^{53}, Ala^{58}, Ala^{61}, and Ala^{62}, which all have <10% solvent exposure. The structure is highly amphiphilic, with the positively charged residues clustering on one surface around the end of helix 4, the start of helix 1, and centrally on helix 2.

Enterocin NKR-5-3B Structural Gene. On the basis of the amino acid sequence of enterocin NKR-5-3B, oligonucleotide primers were designed and employed for PCR sequence analysis to obtain the gene encoding enterocin NKR-5-3B. As a result, the DNA sequence of the gene termed *enkB* and surrounding region was obtained, as shown in Figure 5A. The putative precursor of enterocin NKR-5-3B (EnkB) comprises 87 amino acid residues that include a 23-amino acid N-terminal leader sequence. The calculated mass of the mature peptide moiety with an additional peptide bond with N- and C-terminal residues is 6316.7 Da, which agrees well with the observed mass of enterocin NKR-5-3B. A BLAST search of the peptide sequence translated from the putative *enkB* gene revealed multiple entries of a highly similar putative circular bacteriocin from *E. faecium* that was 90% identical to EnkB (Figure 5B). Furthermore, a BLAST search of the *enkB* putative gene sequence revealed that it is 30 and 20% identical to *ublA* [gene encoding uberolysin A, a circular bacteriocin from *Streptococcus uberis* 42 (15)] and *cirA* [gene encoding circularin A, a circular bacteriocin from *Clostridium beijerinckii* ATCC 25752 (13)], respectively, although direct comparison of the peptide sequence of their entire precursor peptide revealed that EnkB contains a leader sequence (23 amino acids) much longer than that of circularin A (3 amino acids) and uberolysin A (6 amino acids) (Figure 5C).

Serum Stability and Hemolytic Assay. We tested the stability of enterocin NKR-5-3B and found that it is stable in human serum for 24 h (Figure 6A). It had mild hemolytic activity, with a HD_{50} of 6.9 μM (Figure 6B). Because this is higher than the active MIC values for antibacterial activity, hemolysis is unlikely to be a limiting factor in its use as an antibacterial.

Interaction of Enterocin NKR-5-3B with Model Membranes. The interaction of enterocin NKR-5-3B with model membranes was evaluated by SPR. A POPC/chol/SM mixture (molar ratio of 1:1:1) was used to mimic the properties of the cell membrane of red blood cells (RBCs), a POPE/POPG mixture (molar ratio of 7:3) to mimic the membrane properties of Gram-negative cell membranes, and a POPG/CL mixture (molar ratio of 6:4) to mimic Gram-positive bacterial cell membranes. Model membranes composed of a lipid mixture extracted from *E. coli* bacteria were also included. The peptide concentration range used in the peptide−membrane studies was higher than the biological active concentrations because of SPR detection limitations, but this is not expected to affect the interpretation (see Table 2).

Comparison of the sensorgrams at a fixed peptide concentration [16 μM (Figure 7A)] and of the dose−response curves (Figure 7B) showed that the ability of enterocin NKR-5-3B to bind lipid bilayers is dependent on lipid composition. To quantify the differences in affinity, the maximal amount of peptide bound to each lipid system (P/L_{max}) was calculated (Table 5). In particular, the ability to bind to POPG/CL membranes is 24-fold higher than the ability to bind to POPC/Chol/SM membranes and 5-fold higher than the ability to bind to membranes composed of *E. coli* lipid extract or a POPE/POPG mixture. Overall, these results suggest that NKR-5-3B binds only weakly to the neutral membranes that mimic the outer leaflet of RBCs but has a higher affinity for negatively charged membranes that mimic bacterial membranes, in particular membranes that mimic those of Gram-positive bacteria.

DISCUSSION

E. faecium NKR-5-3, isolated from Thai fermented fish, produces five different peptides that are classified as bacteriocins.[24−26] Enterocin NKR-5-3B shows an antimicrobial activity spectrum that is broader than those of the other four NKR-5-3 enterocins (Table 2).[24] Whereas the amino acid sequences of the other four NKR-5-3 enterocins were obtained with relative ease, direct Edman degradation sequencing of enterocin NKR-5-3B did not yield any sequence. We show here that head-to-tail cyclization of enterocin NKR-5-3B precludes sequence analysis by Edman degradation and report the full sequence, 3D solution structure, and gene structure of this novel peptide.

The NMR structure of enterocin NKR-5-3B revealed four helical segments that enclose a tightly packed hydrophobic core, with a head-to-tail ligation of residues Leu^{1} and Trp^{64} forming a circular backbone. The structure is very well-defined in solution, as is evident from the low root-mean-square deviation of the heavy atoms of the backbone and side chains (0.77 Å). The stability of the fold is highlighted by the exceptional protection of amide protons from the solvent. The majority of amide protons involved in hydrogen bonds were found to be slowly exchanging when the protein was reconstituted in D_2O, with a subset not being fully exchanged even after 4 years! Interestingly, the slowly exchanging amides

DOI: 10.1021/acs.biochem.5b00196
Biochemistry 2015, 54, 4863−4876

Table 4. NMR Distances and Dihedral Statistics

no. of distance constraints	
NOE	
total	1048
intraresidual ($\|i - j\| = 0$)	297
sequential ($\|i - j\| = 1$)	274
medium-range ($\|i - j\| \leq 4$)	294
long-range ($\|i - j\| \geq 5$)	183
hydrogen bonds (for 48 H-bonds)	96
no. of dihedral angles	
ϕ	54
ψ	54
χ^1	28
structural statistics	
no. of violations	
distance constraints (>0.2 Å)	0
dihedral angle constraints (>3°)	0
maximum distance constraint violation (Å)	0.176
maximum dihedral angle constraints (deg)	2.3
energy (kcal/mol, mean ± standard deviation)	
overall	−2137 ± 19.3
bond	16.1 ± 0.81
angles	42.4 ± 2.58
improper	20.3 ± 2.16
vdw	−237.4 ± 6.15
NOE (experimental)	0.260 ± 0.017
cDih (experimental)	0.619 ± 0.32
dihedral	279.1 ± 1.15
electric	−2259 ± 15.8
root-mean-square deviation from idealized geometry	
bond lengths (Å)	0.00831 ± 0.00023
bond angles (deg)	0.878 ± 0.021
impropers (deg)	1.12 ± 0.081
average pairwise root-mean-square deviation[a] (Å)	
heavy	0.77 ± 0.10
backbone	0.51 ± 0.14
Molprobity	
Clash score, all atoms[b]	14.4 ± 2.15
poor rotamers	0 ± 0
Ramachandran favored (%)	95.2 ± 1.57
Ramachandran allowed (%)	4.84 ± 1.57
Ramachandran outliers (%)	0 ± 0
Molprobity score	1.97 ± 0.095
Molprobity score percentile[c]	76.9 ± 4.46
CB deviations, bad backbone bonds/angles	0 ± 0

[a]Pairwise root-mean-square deviation from 20 refined structures over amino acids 1−64. [b]Number of steric overlaps (>0.4 Å) per 1000 atoms. [c]A value of 100% is the best among structures of comparable resolution; 0% is the worst.

are spread throughout the helical regions, including around the cyclization site in helix 4, suggesting that all helices are very stable. In contrast to the core region, two of the surface loops comprising residues 22−24 and 37−42 are highly dynamic, as is evident from chemical shift analyses. These loops comprise small polar residues, including Gly and Ser, which probably contributes to their flexibility.

The high stability of enterocin NKR-5-3B is evident from data showing retained activity following high-temperature and low-pH treatments. High stability is a feature common to all backbone-cyclic peptides; however, unlike plant-derived cyclotides, which contain internal disulfide bridges that enhance their stability,[9,42] circular bacteriocins (bacterial origin), except subtilosin A, which is cross-braced by thioether bonds,[12] do not contain internal bridges.[5,7] Thus, we can conclude that for the larger bacteriocins the combination of a substantial hydrophobic core and a circular backbone is sufficient to ensure an ultrastable structure. The importance of the circular backbone for the stability of the circular bacteriocin enterocin AS-48 has been demonstrated by Montalban-Lopez and colleagues.[43] Linear forms of enterocin AS-48 obtained by enzymatic digestion had thermal stress resistance lower than that of the cyclic peptide and were highly susceptible to freeze−thaw stress.

It has previously been suggested that the family of circular bacteriocins shares a common structural fold, the so-called saposin fold.[22] This fold refers to a structural motif found in a family of bioactive polypeptides that contain five α-helices

DOI: 10.1021/acs.biochem.5b00196
Biochemistry 2015, 54, 4863−4876

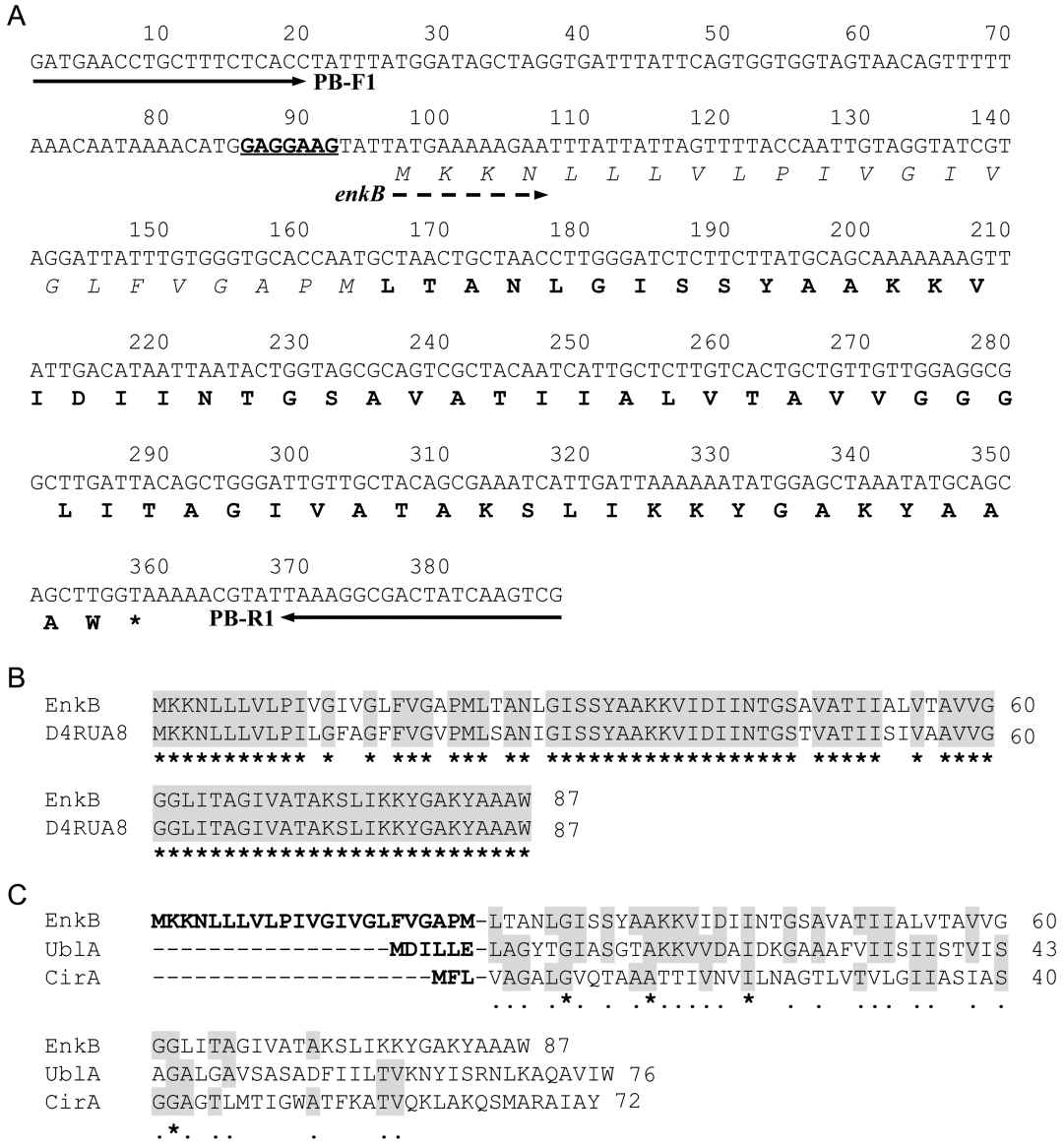

Figure 5. (A) Nucleotide sequence of the region encoding the structural gene of enterocin NKR-5-3B. The start codon of the precursor peptide of enterocin NKR-5-3B is indicated by a dotted arrow. Enterocin NKR-5-3B specific primers are indicated by a solid arrow. A putative ribosome binding site and a stop codon are underlined and denoted with an asterisk, respectively. The deduced amino acid sequence is indicated below the nucleotide sequence, where the sequence corresponding to the mature enterocin NKR-5-3B peptide is shown in bold. (B and C) Alignment of the enterocin NKR-5-3B precursor peptide with predicted proteins from *E. faecium*. (B) BLAST searching of the elucidated sequence of the enterocin NKR-5-3B precursor peptide (EnkB) revealed 90% sequence identity to Uniprot entries D4RUA8 (as well as D4RGC3, D0ARJ8, D0AJL7, C9C5V8, and C9BRP5, all of which were identical). (C) Alignment of the precursor peptides of enterocin NKR-5-3B with other circular bacteriocins (uberolysin A, UblA; circularin A, CirA) deduced from their structural genes (*ublA*, 30%; *cirA*, 20%), revealing the difference in the length of their leader sequence (highlighted in bold). Conserved and semiconserved residues are denoted with an asterisk and a colon, respectively. Identical residues are highlighted in gray.

folded into a globular domain with a hydrophobic core and a hydrophilic surface.[44] Although the two bacteriocins structurally characterized to date, enterocin AS-48 and carnocyclin A, differ in that carnocyclin A has only four helices, the helical segments reside in similar positions.[22] As shown in Figure 8, the structure of enterocin NKR-5-3B is remarkably similar to that of carnocyclin A, despite having a very low level of amino acid sequence homology, and differing in length by four residues (enterocin NKR-5-3B has 64 residues and carnocyclin A 60 residues). All four helices of enterocin NKR-5-3B superimpose well with respect to the four helices of carnocyclin A. Enterocin AS-48 comprises 70 residues and includes a fifth helical segment. Interestingly, again helices 1−3 superimpose well with enterocin NKR-5-3B and carnocyclin A, whereas the fourth helical segment is replaced with two helices to accommodate the six additional residues, while retaining the overall fold. This strongly supports the idea that all circular bacteriocins have a conserved fold.[22] Furthermore, not only the folds but also the charge distributions of enterocin NKR-5-3B, carnocyclin A, and enterocin AS-48 are highly conserved, as shown in Figure 8. Enterocin NKR-5-3B has a net charge of +5, resulting from six Lys residues and an Asp residue, and carnocyclin A has a net charge of +4, resulting from five Lys residues and a Glu residue. In contrast, enterocin AS-48 is more

DOI: 10.1021/acs.biochem.5b00196
Biochemistry 2015, 54, 4863−4876

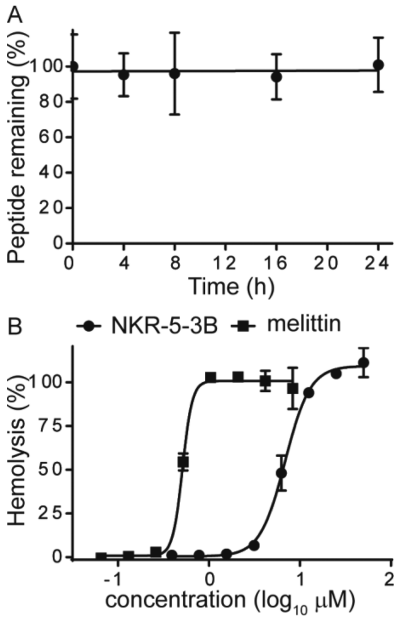

Figure 6. Enterocin NKR-5-3B stability and hemolytic activity. (A) Graph showing the stability of enterocin NKR-5-3B in human serum, with data represented as the percentage of peptide remaining after 24 h. (B) Graph illustrating the percentage of hemolysis of enterocin NKR-5-3B with melittin included as a positive control. Melittin is the principle active component peptide of bee venom. Hemolysis of a human red blood cell was measured as the absorbance at 415 nm. All data are given as means ± the standard deviation.

polar, with eight Lys, two Arg, and four Glu residues, but nonetheless has a similar net charge of +6.

Although the mechanistic details of the mode of action of enterocin NKR-5-3B are yet to be described, it is tempting to surmise that all large circular bacteriocins might have a similar mode of action resulting from their conserved highly amphipathic nature. The mechanism driving the antimicrobial activity of other circular bacteriocins requires insertion into the bacterial cell membrane, either directly[45−49] or through a docking molecule.[50] The strong affinity of enterocin NKR-5-3B for negatively charged membranes (Figure 7) illustrates its possible electrostatic interaction-driven mode of action caused by its highly cationic cluster that probably facilitates its initial approach to the negatively charged membrane. Most circular bacteriocins have a high net positive charge and are believed to nonselectively bind to the target membrane based on such electrostatic interactions. The broader antimicrobial activities of enterocin NKR-5-3B and other circular bacteriocins compared with those of other types of bacteriocins are in agreement with this hypothesis, given their well-defined structures and surface presentation of positively charged residues. As more sequences of circular bacteriocins become available, future bioinformatic approaches, including homology modeling and prediction of modes of target recognition, may further assist in elucidating their modes of action. The 3D structure determined here provides an experimental template for guiding such future studies.

Gram-positive bacteria possess a higher percentage of negatively charged lipids in their inner membrane than Gram-negative bacteria. The higher affinity of enterocin NKR-5-3B for model membranes that mimic Gram-positive bacteria, compared to its affinity for model membranes that mimic Gram-negative bacteria, is in agreement with its higher antimicrobial activity toward Gram-positive strains and suggests that electrostatic attractions and the ability to bind to the bacterial membrane are important for its activity. The low affinity of NKR-5-3B for zwitterionic model membranes that mimic RBC membranes (Figure 7) further supports the importance of electrostatic interactions in its activity. Among the family of circular bacteriocins, the mode of action of enterocin AS-48 on a molecular level is arguably the best understood. It is thought that enterocin AS-48 in its water-soluble form electrostatically approaches the target membrane surface, after which it uses its exposed hydrophobic face to facilitate insertion into the target membrane via molecular electroporation and hydrophobic interactions.[21,46,51,52] In addition to electrostatic and hydrophobic interactions as possible driving forces to attract NKR-5-3B to the bacterial cell surface, the selectivity and high potency toward Gram-positive bacteria might result from a receptor on the cell membrane that further facilitates the action of enterocin NKR-5-3B, as in the case of another circular bacteriocin, garvicin ML, which utilizes the maltose ABC transporter for its action.[50]

Although much is known about the biosynthetic mechanism of other classes of bacteriocins (for example, class I and class IIa), the biosynthetic mechanism for the production of circular bacteriocins still remains a mystery. As in the case of carnocyclin A and enterocin AS-48, the ligation site joining the N- and C-termini of enterocin NKR-5-3B is located within a helical segment (helix 4), which spans residues 58−65. This region is composed mainly of hydrophobic residues (Figure 3). Although the enzymatic mechanism of head-to-tail ligation of circular bacteriocins is yet to be uncovered, it has been inferred that the hydrophobic patches surrounding the point of head-to-

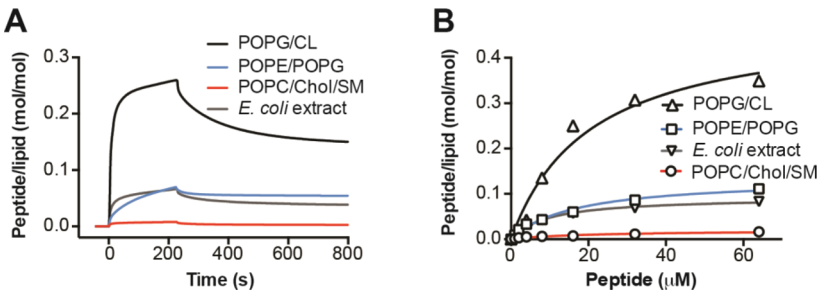

Figure 7. Interaction of enterocin NKR-5-3B with model membranes followed by SPR. (A) Sensorgrams obtained with 16 μM enterocin NKR-5-3B or (B) dose−response curves over POPC/Chol/SM (1:1:1), POPE/POPG (7:3), or POPG/CL (6:4) bilayers or *E. coli* polar lipid extract deposited onto an L1 chip sensor. The signal was converted into the peptide-to-lipid molar ratio as previously described.[40] Curves were fitted with a saturation binding curve (see the parameters in Table 5).

DOI: 10.1021/acs.biochem.5b00196
Biochemistry 2015, 54, 4863−4876

Table 5. Affinities of NKR-5-3B for Lipid Membranes Followed by SPR[a]

	POPC/Chol/SM	POPE/POPG	POPG/CL	*E. coli* extract
P/L_{max}	0.020 ± 0.003	0.135 ± 0.010	0.484 ± 0.061	0.093 ± 0.003
k_d (μM)	20.9 ± 7.3	16.5 ± 3.0	20.4 ± 6.2	9.4 ± 1.0

[a]Dose−response curves shown in Figure 7B were fitted with a saturation binding curve: $P/L = (P/L_{max} \times [\text{peptide}])/(k_d + [\text{peptide}])$, where P/L is the peptide-to-lipid ratio, P/L_{max} is the P/L maximum, and k_d is the peptide concentration required to achieve half of P/L_{max}.

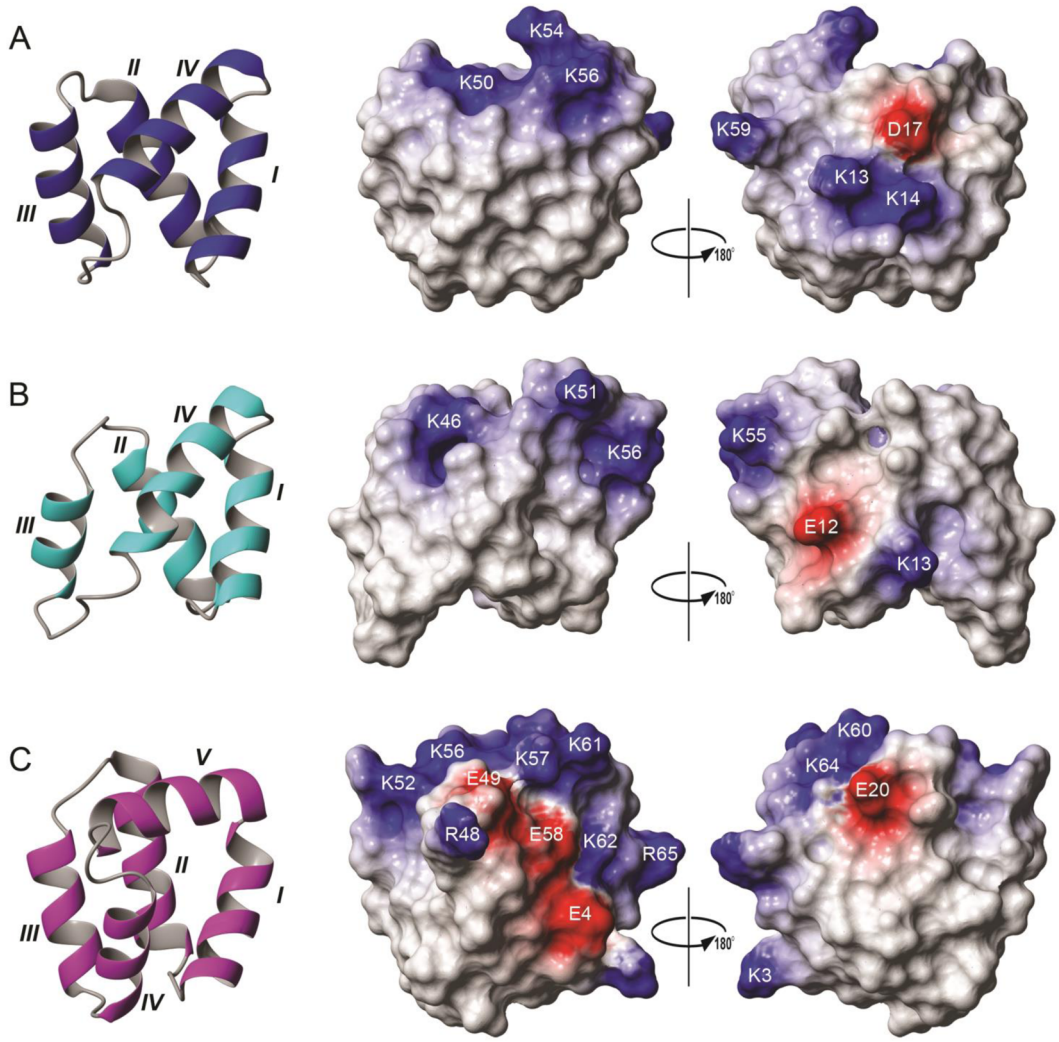

Figure 8. Comparison of enterocin NKR-5-3B with carnocyclin A and enterocin AS-48. The structures of enterocin NKR-5-3B (A) and carnocyclin A (B) both possess four helical segments, with a remarkably similar arrangement. Enterocin AS-48 (C) comprises a fifth helix but has a similar overall fold. The charge distribution of the three peptides is also highly conserved, despite significant differences in the number of charged residues. The helical segments are labeled with Roman numerals. The surface views are rotated 180° relative to each other. Positive charges are colored blue and negative charges red. All charged residues are labeled with single-amino acid codes and residue numbers.

tail ligation play a role in the interaction between processing enzyme(s) and the linear precursor peptide to yield the mature circular bacteriocin.[22] The flexible loops connecting helical regions are also likely to be critical for the folding and cyclization of enterocin NKR-5-3B, allowing the helical segments to move into position and bring the termini into proximity for the cyclization event.

As mentioned above, although members of the family of circular bacteriocins share very little consensus in their leader sequences, their mature peptide region shares a common structural conformation.[22] It is tempting to speculate that the structures of their propeptides encode information regarding the molecular mechanism of the ligation of their N- and C-termini. Thus, 3D structural information for these peptides may help in revealing the substrate region for the active site of their biosynthetic enzymes. Although much remains to be learned about the biosynthetic process, the two key structural findings that (i) ligation occurs at a site that forms a "new" helix that cannot have existed in the precursor protein (because it is formed from discontinuous elements) and (ii) other helices in the structure are linked with flexible loops, thereby allowing positioning of the termini for ligation, provide some insights into the mechanism.

The suite of putative circular bacteriocins with a very high level of identity to enterocin NKR-5-3B implies that there could be many more natural variants of this circular bacteriocin that

DOI: 10.1021/acs.biochem.5b00196
Biochemistry 2015, 54, 4863−4876

exist in strains that are close to *E. faecium* in evolutionary history. Genetic information regarding the homology of the *enkB* gene to other circular bacteriocins should be helpful in the future for the process of identifying its biosynthetic genes encoding the enzymes responsible for its maturation (cyclization).

In conclusion, we have shown here that enterocin NKR-5-3B belongs to the class IIc family of circular bacteriocins. Its 3D structure provides strong evidence of the idea that larger peptides of this family share a highly conserved fold, despite diverse primary sequences. The conserved structure and charge distribution provide insights into its mode of action and a basis for more detailed mechanistic studies. Specifically, the structural information reported here reveals that, as for carnocyclin A and enterocin AS-48, the site of cyclization is located in the middle of a helical segment, and thus, cyclization is probably required for the peptide to adopt its 3D structure. Finally, the identification of the gene encoding enterocin NKR-5-3B reported here highlights the differences in the nature and size of the leader peptides of cyclic bacteriocins and will be helpful for further studies of this circular bacteriocin, including the identification of the enzymes responsible for its biosynthesis. Searches using the gene information for NKR-5-3B identified other highly conserved peptides in *E. faecium* and less conserved peptides in other bacterial species, suggesting the circular bacteriocin family is a rich and untapped source of novel antimicrobial peptides valuable for applications in human health and food safety.

AUTHOR INFORMATION

Corresponding Author

*Laboratory of Microbial Technology, Department of Bioscience and Biotechnology, Faculty of Agriculture, Kyushu University, 6-10-1 Hakozaki, Higashi-ku, Fukuoka 812-8581, Japan. Telephone and fax: (+81) 92-642-3019. E-mail: sonomoto@agr.kyushu-u.ac.jp.

Funding

D.J.C. is a National Health and Medical Research Council (NHMRC) Professorial Research Fellow (APP1026501). Work in his laboratory on circular proteins is supported by a grant from the Australian Research Council (DP150100443). K.J.R. is an ARC Future Fellow. N.I. is a JSPS Fellow. S.T.H. is supported by a Discovery Early Career Research Award from ARC. This work was partially supported by JSPS KAKENHI Grant 24380051, the Kato Memorial Bioscience Foundation, and the Novozymes Japan Research Fund.

Notes

The authors declare no competing financial interest.

ACKNOWLEDGMENTS

We thank the Molecular & Cellular Proteomics Mass Spectrometry Facility and the Queensland NMR Network for access to instrumentation and the JSPS-NRCT Core University Program on "Development of Thermo-tolerant Microbial Resources and Their Applications" for the collaboration between Japan and Thailand.

ABBREVIATIONS

LAB, lactic acid bacteria; MDR, multidrug resistant; MIC, minimum inhibitory concentration.

REFERENCES

(1) Cleveland, J., Montville, T. J., Nes, I. F., and Chikindas, M. L. (2001) Bacteriocins: safe, natural antimicrobials for food preservation. *Int. J. Food Microbiol. 71*, 1−20.

(2) Chen, H., and Hoover, D. G. (2003) Bacteriocins and their food applications. *Compr. Rev. Food Sci. Food Saf. 2*, 82−100.

(3) Cotter, P. D., Hill, C., and Ross, R. P. (2005) Bacteriocins: developing innate immunity for food. *Nat. Rev. Microbiol. 3*, 777−788.

(4) Cotter, P. D., Ross, R. P., and Hill, C. (2012) Bacteriocins − a viable alternative to antibiotics? *Nat. Rev. Microbiol. 11*, 95−105.

(5) Masuda, Y., Zendo, T., and Sonomoto, K. (2012) New type of non-lantibiotic bacteriocins: circular and leaderless bacteriocins. *Benefic. Microbes 3*, 3−12.

(6) Maqueda, M., Sanchez-Hidalgo, M., Fernandez, M., Montalban-Lopez, M., Valdivia, E., and Martinez-Bueno, M. (2008) Genetic features of circular bacteriocins produced by Gram-positive bacteria. *FEMS Microbiol. Rev. 32*, 2−22.

(7) van Belkum, M. J., Martin-Visscher, L. A., and Vederas, J. C. (2011) Structure and genetics of circular bacteriocins. *Trends Microbiol. 19*, 411−418.

(8) Conlan, B. F., Gillon, A. D., Craik, D. J., and Anderson, M. A. (2010) Circular proteins and mechanisms of cyclization. *Biopolymers 94*, 573−583.

(9) Craik, D. J., Mylne, J. S., and Daly, N. L. (2010) Cyclotides: macrocyclic peptides with applications in drug design and agriculture. *Cell. Mol. Life Sci. 67*, 9−16.

(10) Galvez, A., Maqueda, M., Valdivia, E., Quesada, A., and Montoya, E. (1986) Characterization and partial purification of a broad spectrum antibiotic AS-48 produced by *Streptococcus faecalis*. *Can. J. Microbiol. 32*, 765−771.

(11) Kawai, Y., Saito, T., Kitazawa, H., and Itoh, T. (1998) Gassericin A; an uncommon cyclic bacteriocin produced by *Lactobacillus gasseri* LA39 linked at N- and C-terminal ends. *Biosci., Biotechnol., Biochem. 62*, 2438−2440.

(12) Kawulka, K., Sprules, T., McKay, R. T., Mercier, P., Diaper, C. M., Zuber, P., and Vederas, J. C. (2003) Structure of subtilosin A, an antimicrobial peptide from *Bacillus subtilis* with unusual posttranslational modifications linking cysteine sulfurs to alpha-carbons of phenylalanine and threonine. *J. Am. Chem. Soc. 125*, 4726−4727.

(13) Kemperman, R., Kuipers, A., Karsens, H., Nauta, A., Kuipers, O., and Kok, J. (2003) Identification and characterization of two novel clostridial bacteriocins, circularin A and closticin 574. *Appl. Environ. Microbiol. 69*, 1589−1597.

(14) Kalmokoff, M. L., Cyr, T. D., Hefford, M. A., Whitford, M. F., and Teather, R. M. (2003) Butyrivibriocin AR10, a new cyclic bacteriocin produced by the ruminal anaerobe *Butyrivibrio fibrisolvens* AR10: characterization of the gene and peptide. *Can. J. Microbiol. 49*, 763−773.

(15) Wirawan, R. E., Swanson, K. M., Kleffmann, T., Jack, R. W., and Tagg, J. R. (2007) Uberolysin: a novel cyclic bacteriocin produced by *Streptococcus uberis*. *Microbiology 153*, 1619−1630.

(16) Martin-Visscher, L. A., van Belkum, M. J., Garneau-Tsodikova, S., Whittal, R. M., Zheng, J., McMullen, L. M., and Vederas, J. C. (2008) Isolation and characterization of carnocyclin A, a novel circular bacteriocin produced by *Carnobacterium maltaromaticum* UAL307. *Appl. Environ. Microbiol. 74*, 4756−4763.

(17) Sawa, N., Zendo, T., Kiyofuji, J., Fujita, K., Himeno, K., Nakayama, J., and Sonomoto, K. (2009) Identification and characterization of lactocyclicin Q, a novel cyclic bacteriocin produced by *Lactococcus* sp. strain QU 12. *Appl. Environ. Microbiol. 75*, 1552−1558.

(18) Borrero, J., Brede, D. A., Skaugen, M., Diep, D. B., Herranz, C., Nes, I. F., Cintas, L. M., and Hernandez, P. E. (2011) Characterization of garvicin ML, a novel circular bacteriocin produced by *Lactococcus garvieae* DCC43, isolated from mallard ducks (*Anas platyrhynchos*). *Appl. Environ. Microbiol. 77*, 369−373.

(19) Masuda, Y., Ono, H., Kitagawa, H., Ito, H., Mu, F., Sawa, N., Zendo, T., and Sonomoto, K. (2011) Identification and characterization of leucocyclicin Q, a novel cyclic bacteriocin produced by

DOI: 10.1021/acs.biochem.5b00196
Biochemistry 2015, 54, 4863−4876

Leuconostoc mesenteroides TK41401. *Appl. Environ. Microbiol. 77*, 8164−8170.
(20) Kawulka, K. E., Sprules, T., Diaper, C. M., Whittal, R. M., McKay, R. T., Mercier, P., Zuber, P., and Vederas, J. C. (2004) Structure of subtilosin A, a cyclic antimicrobial peptide from *Bacillus subtilis* with unusual sulfur to alpha-carbon cross-links: formation and reduction of alpha-thio-alpha-amino acid derivatives. *Biochemistry 43*, 3385−3395.
(21) Gonzalez, C., Langdon, G. M., Bruix, M., Galvez, A., Valdivia, E., Maqueda, M., and Rico, M. (2000) Bacteriocin AS-48, a microbial cyclic polypeptide structurally and functionally related to mammalian NK-lysin. *Proc. Natl. Acad. Sci. U. S. A. 97*, 11221−11226.
(22) Martin-Visscher, L. A., Gong, X., Duszyk, M., and Vederas, J. C. (2009) The three-dimensional structure of carnocyclin A reveals that many circular bacteriocins share a common structural motif. *J. Biol. Chem. 284*, 28674−28681.
(23) Wilaipun, P., Zendo, T., Sangjindavong, M., Nitisinprasert, S., Leelawatcharamas, V., Nakayama, J., and Sonomoto, K. (2004) The two-synergistic peptide bacteriocin produced by *Enterococcus faecium* NKR-5−3 isolated from Thai fermented fish (*Pla-ra*). *ScienceAsia 30*, 115−122.
(24) Ishibashi, N., Himeno, K., Fujita, K., Masuda, Y., Perez, R. H., Zendo, T., Wilaipun, P., Leelawatcharamas, V., Nakayama, J., and Sonomoto, K. (2012) Purification and characterization of multiple bacteriocins and an inducing peptide produced by *Enterococcus faecium* NKR-5−3 from Thai fermented fish. *Biosci., Biotechnol., Biochem. 76*, 947−953.
(25) Himeno, K., Fujita, K., Zendo, T., Wilaipun, P., Ishibashi, N., Masuda, Y., Yoneyama, F., Leelawatcharamas, V., Nakayama, J., and Sonomoto, K. (2012) Identification of enterocin NKR-5−3C, a novel class IIa bacteriocin produced by a multiple bacteriocin producer. *Biosci., Biotechnol., Biochem. 76*, 1245−1247.
(26) Perez, R. H., Himeno, K., Ishibashi, N., Masuda, Y., Zendo, T., Fujita, K., Wilaipun, P., Leelawatcharamas, V., Nakayama, J., and Sonomoto, K. (2012) Monitoring of the multiple bacteriocin production by *Enterococcus faecium* NKR-5−3 through a developed liquid chromatography and mass spectrometry-based quantification system. *J. Biosci. Bioeng. 114*, 490−496.
(27) Siragusa, G. R., and Cutter, C. N. (1993) Brochocin-C, a new bacteriocin produced by *Brochothrix campestris*. *Appl. Environ. Microbiol. 59*, 2326−2328.
(28) Sambrook, J., and Russell, D. W. (2001) *Molecular cloning: A laboratory manual*, 3rd ed., Cold Spring Harbor Laboratory Press, Plainview, NY.
(29) Ennahar, S., Sashihara, T., Sonomoto, K., and Ishizaki, A. (2000) Class IIa bacteriocins: biosynthesis, structure and activity. *FEMS Microbiol. Rev. 24*, 85−106.
(30) Saska, I., Colgrave, M. L., Jones, A., Anderson, M. A., and Craik, D. J. (2008) Quantitative analysis of backbone-cyclised peptides in plants. *J. Chromatogr. B: Anal. Technol. Biomed. Life Sci. 872*, 107−114.
(31) Keller, R. L. J. (2004) *The computer aided resonance assignment tutorial*, Cantina Verlag, Goldau, Switzerland.
(32) Shen, Y., and Bax, A. (2013) Protein backbone and sidechain torsion angles predicted from NMR chemical shifts using artificial neutral networks. *J. Biomol. NMR 56*, 227−241.
(33) Güntert, P. (2004) Automated NMR structure calculation with CYANA. *Methods Mol. Biol. 278*, 353−378.
(34) Brunger, A. T. (2007) Version 1.2 of the Crystallography and NMR System. *Nat. Protoc. 2*, 2728−2733.
(35) Nederveen, A. J., Doreleijers, J. F., Vranken, W., Miller, Z., Spronk, C. A. E. M., Nabuurs, S. B., Güntert, P., Livny, M., Markley, J. L., Nilges, M., Ulrich, E. L., Kaptein, R., and Bonvin, A. M. J. J. (2005) RECOORD: A recalculated coordinate database of 500+ proteins from the PDB using restraints from the BioMagResBank. *Proteins: Struct., Funct., Genet. 59*, 662−672.
(36) Davis, I. W., Leaver-Fay, A., Chen, V. B., Block, J. N., Kapral, G. J., Wang, X., Murray, L. W., Arendall, W. B., 3rd, Snoeyink, J., Richardson, J. S., and Richardson, D. C. (2007) MolProbity: all-atom contacts and structure validation for proteins and nucleic acids. *Nucleic Acids Res. 35*, W375−W383.
(37) Koradi, R., Billeter, M., and Wüthrich, K. (1996) MOLMOL: A program for display and analysis of macromolecular structures. *J. Mol. Graphics 14*, 51−55.
(38) Fujita, K., Ichimasa, S., Zendo, T., Koga, S., Yoneyama, F., Nakayama, J., and Sonomoto, K. (2007) Structural analysis and characterization of lacticin Q, a novel bacteriocin belonging to a new family of unmodified bacteriocins of Gram-positive bacteria. *Appl. Environ. Microbiol. 73*, 2871−2877.
(39) Chan, L. Y., Gunasekera, S., Henriques, S. T., Worth, N. F., Le, S. J., Clark, R. J., Campbell, J. H., Craik, D. J., and Daly, N. L. (2011) Engineering pro-angiogenic peptides using stable disulfide-rich cyclic scaffolds. *Blood 118*, 6709−6717.
(40) Henriques, S. T., Huang, Y. H., Castanho, M. A. R. B., Bagatolli, L. A., Sonza, S., Tachedjian, G., Daly, N. L., and Craik, D. J. (2012) Phosphatidylethanolamine binding is a conserved feature of cyclotide-membrane interactions. *J. Biol. Chem. 287*, 33629−33643.
(41) Berjanskii, M. V., and Wishart, D. S. (2005) A simple method to predict protein flexibility using secondary chemical shifts. *J. Am. Chem. Soc. 127*, 14970−14971.
(42) Jagadish, K., and Camarero, J. A. (2010) Cyclotides, a promising molecular scaffold for peptide-based therapeutics. *Biopolymers 94*, 611−616.
(43) Montalban-Lopez, M., Spolaore, B., Pinato, O., Martinez-Bueno, M., Valdivia, E., Maqueda, M., and Fontana, A. (2008) Characterization of linear forms of the circular enterocin AS-48 obtained by limited proteolysis. *FEBS Lett. 582*, 3237−3242.
(44) Liepinsh, E., Andersson, M., Ruysschaert, J. M., and Otting, G. (1997) Saposin fold revealed by the NMR structure of NK-lysin. *Nat. Struct. Biol. 4*, 793−795.
(45) Kawai, Y., Ishii, Y., Arakawa, K., Uemura, K., Saitoh, B., Nishimura, J., Kitazawa, H., Yamazaki, Y., Tateno, Y., Itoh, T., and Saito, T. (2004) Structural and functional differences in two cyclic bacteriocins with the same sequences produced by Lactobacilli. *Appl. Environ. Microbiol. 70*, 2906−2911.
(46) Sanchez-Barrena, M. J., Martinez-Ripoll, M., Galvez, A., Valdivia, E., Maqueda, M., Cruz, V., and Albert, A. (2003) Structure of bacteriocin AS-48: from soluble state to membrane bound state. *J. Mol. Biol. 334*, 541−549.
(47) Gong, X., Martin-Visscher, L. A., Nahirney, D., Vederas, J. C., and Duszyk, M. (2009) The circular bacteriocin, carnocyclin A, forms anion-selective channels in lipid bilayers. *Biochim. Biophys. Acta, Biomembr. 1788*, 1797−1803.
(48) Thennarasu, S., Lee, D. K., Poon, A., Kawulka, K. E., Vederas, J. C., and Ramamoorthy, A. (2005) Membrane permeabilization, orientation, and antimicrobial mechanism of subtilosin A. *Chem. Phys. Lipids 137*, 38−51.
(49) Galvez, A., Maqueda, M., Martinez-Bueno, M., and Valdivia, E. (1991) Permeation of bacterial cells, permeation of cytoplasmic and artificial membrane vesicles, and channel formation on lipid bilayers by peptide antibiotic AS-48. *J. Bacteriol. 173*, 886−892.
(50) Gabrielsen, C., Brede, D. A., Hernandez, P. E., Nes, I. F., and Diep, D. B. (2012) The maltose ABC transporter in *Lactococcus lactis* facilitates high-level sensitivity to the circular bacteriocin garvicin ML. *Antimicrob. Agents Chemother. 56*, 2908−2915.
(51) Jimenez, M. A., Barrachi-Saccilotto, A. C., Valdivia, E., Maqueda, M., and Rico, M. (2005) Design, NMR characterization and activity of a 21-residue peptide fragment of bacteriocin AS-48 containing its putative membrane interacting region. *J. Pept. Sci. 11*, 29−36.
(52) Maqueda, M., Galvez, A., Bueno, M. M., Sanchez-Barrena, M. J., Gonzalez, C., Albert, A., Rico, M., and Valdivia, E. (2004) Peptide AS-48: prototype of a new class of cyclic bacteriocins. *Curr. Protein Pept. Sci. 5*, 399−416.
(53) Wishart, D. S., and Sykes, B. D. (1994) The ^{13}C chemical-shift index: A simple method for the identification of protein secondary structure using ^{13}C chemical-shift data. *J. Biomol. NMR 4*, 171−180.

DOI: 10.1021/acs.biochem.5b00196
Biochemistry 2015, 54, 4863−4876